

## Determination of the $^{29}\text{Si}$ level density from 3 to 22 MeV

F. B. Bateman,<sup>\*</sup> S. M. Grimes, N. Boukharouba,<sup>†</sup> V. Mishra,<sup>‡</sup> C. E. Brient, R. S. Pedroni,<sup>§</sup> and T. N. Massey  
*Institute of Nuclear and Particle Physics, Ohio University, Athens, Ohio 45701*

R. C. Haight

*Los Alamos National Laboratory, Los Alamos, New Mexico 87545*

(Received 28 September 1995; revised manuscript received 2 August 1996)

The level density of  $^{29}\text{Si}$  has been studied over an excitation energy range of 3 to 22 MeV. Three techniques were used to derive level density values from experimental data. In the region of resolved levels, results were obtained from level counting while neutron resonance data were used in the region of slightly overlapping levels near the neutron binding energy. At the highest excitation energies, characterized by strongly overlapping levels, Ericson theory was employed to deduce level densities by examining energy-dependent fluctuations in cross sections. Three reactions yielding the same compound nucleus,  $^{29}\text{Si}$ , were investigated. Partial cross sections from  $^{28}\text{Si}(n,p)$ ,  $^{28}\text{Si}(n,\alpha)$ , and  $^{27}\text{Al}(d,n)^{28}\text{Si}$  reactions were measured with good experimental resolution and statistical accuracy. From these cross sections, level densities were extracted using the two independent methods proposed by Ericson. Reasonable agreement was found among level densities derived from the two Ericson methods. Values obtained are also fairly consistent with those of various predictions and theoretical models. [S0556-2813(97)05201-1]

PACS number(s): 21.10.Ma, 24.60.Ky, 25.40.Lw, 27.30.+t

### I. INTRODUCTION

Determination of level densities is vital to many areas of basic and applied nuclear research. Level densities represent a crucial input ingredient of Hauser-Feshbach calculations and are therefore relevant to astrophysical nucleosynthesis calculations as well as fission and fusion energy research. As a basic concept, the nuclear level density is an important facet of the structure of quantum mechanical many-body systems with isospin. Over the years, much theoretical and experimental work has been conducted in an effort to explain level density systematics. Although these efforts have met with success in describing general tendencies, a detailed understanding is still lacking.

Several experimental techniques exist for the measurement of level densities. The choice of a particular method is usually dictated by the excitation energy reached in the compound nucleus. At the lowest excitation energies, level densities can be derived using a simple counting technique based on tabulated energy levels. This method is limited to the first few MeV of excitation energy, beyond which levels become unresolved. A rich source of level density information is provided by resonance data at excitation energies slightly above the neutron and proton binding energies. Provided a reaction is nonselective and experimental resolution is good enough to resolve individual levels, compound nuclear level den-

sities can be obtained from the number of resonances in an energy interval.

At higher excitation energies where levels begin to overlap, evaporation spectra are commonly used to measure level densities via the Hauser-Feshbach formalism. The shape of evaporation spectra can provide information about the form of the level density function. Although the cross sections are usually large, their smooth spectral shape makes estimation of backgrounds difficult. Absolute normalization is generally required using one of the other methods. At very high excitation energies, level widths can be much larger than the average level spacing ( $\Gamma \gg D$ ). In this region of strongly overlapping levels, cross sections can fluctuate rapidly with bombarding energy. Ericson theory provides a method for determining level densities via a statistical analysis of energy variations in excitation functions. Since evaporation spectra include contributions from multistep reactions at these energies, Ericson fluctuations are virtually the only experimental technique for measuring the level density above 15 MeV. These measurements generally require good energy resolution and many data points to yield reliable level density information.

Ericson [1] has shown that statistical theory allows the prediction not only of average cross sections but also of variances in the energy dependence of cross sections for reactions proceeding through a compound nucleus. According to Ericson, fluctuations in cross sections in the region of overlapping levels can be explained by interference effects, even when the level density is so high that fluctuations in level density can be ignored. By performing a statistical analysis of the variation with energy of the cross sections, information on compound nuclear level densities can be deduced. Two independent techniques for determining level densities are contained in the Ericson theory. These are discussed in detail in Ref. [2]. One method relates the level density to the variance of the cross section (variance method). The other

<sup>\*</sup>Present address: Los Alamos National Laboratory, Los Alamos, NM 87545.

<sup>†</sup>Present address: 1 Rue Ben Brouk Hocine, Heliopolis, Guecma, Algeria.

<sup>‡</sup>Present address: Department of Radiation Oncology, University of Miami Medical School, P.O. Box 016960, Miami, FL 33101.

<sup>§</sup>Present address: 132 28th Ave. South, Jacksonville Beach, FL 32250.

technique expresses the exit channel transmission coefficient in terms of the partial decay width and level spacing of the compound nucleus (width method).

Most of the information on the level density of  $^{29}\text{Si}$  prior to this study has been obtained from neutron total cross section data [2,3]. One of the first measurements of the  $^{29}\text{Si}$  level density derived from partial cross sections was completed by Grimes using a monoenergetic  $D(d,n)$  source [4]. In the current approach, one measurement utilized the Los Alamos Meson Physics Facility (LAMPF) Weapons Neutron Research (WNR) spallation neutron source to measure partial  $(n,z)$  cross sections over a continuous energy range. White neutron sources offer the clear advantage of allowing the simultaneous measurement of excitation functions over all energies while eliminating energy straggling in gas cell foils. Although partial cross sections are by their nature more difficult to measure than total cross sections, they exhibit more pronounced energy fluctuations with energy making an Ericson analysis possible with poorer statistical accuracy. A second measurement utilized the  $^{27}\text{Al}(d,n)^{28}\text{Si}$  reaction, which allowed the analysis to be extended to higher energies.

It should be noted that although the Ericson fluctuations of reactions proceeding through the  $^{29}\text{Si}$  compound nucleus have been studied previously, often the data have not been processed to yield the maximum information about level densities. In some cases, the focus was on determining whether the observed fluctuations had the characteristics predicted by Ericson. These papers often only quote the observed width after authors deduce level densities at particular energies but do not attempt a fit over a wide energy range. It was suggested by the authors of Ref. [2] that, although the total cross section could easily be measured precisely, partial cross sections had larger fluctuations and allowed a better test of some of the parameters which enter the analysis. For these reasons, it was felt that a measurement spanning a range of energies and involving more than one reaction channel would yield considerable information. In addition to the Ericson fluctuation points, level densities deduced from level counting at low energies were also included in the fits.

## II. EXPERIMENTAL DETAILS

To facilitate an Ericson analysis, two experiments yielding the same compound nucleus,  $^{29}\text{Si}$ , were performed. The first of these involves the measurement of partial cross sections resulting from neutron-induced charged-particle-producing reactions on  $^{28}\text{Si}$ . Data were obtained at the WNR facility of the LAMPF. The measurement consisted of the detection of charged particles resulting from neutron bombardment of Si using surface barrier detectors. Upon completion of the  $(n,p)$  and  $(n,\alpha)$  measurements, a second experiment was carried out at Ohio University to improve our knowledge of the  $^{29}\text{Si}$  level density at higher excitation energies. This experiment utilized a 4.5 MV tandem Van de Graaff accelerator producing a beam of deuterons. The deuteron beam was made to strike an  $^{27}\text{Al}$  target. Neutrons resulting from  $(d,n)$  reactions were then detected with NE213 liquid scintillator detectors. Detailed descriptions of the two experiments are presented in the following sections.

### A. $^{28}\text{Si}(n,z)$ measurements at WNR

The pulsed, ‘‘white’’ neutron source for these measurements was provided by the WNR facility at LAMPF [5]. An intense neutron source results when a pulsed beam of 800 MeV protons possessing a burst width of less than 1 ns strikes a tungsten target. The resulting neutron spectrum ranged in energy from a few keV to the primary energy minus the  $(p,n)$   $Q$  value, with most of the flux concentrated between 1 and 300 MeV. For this measurement, only the range  $5 \leq E_n \leq 14$  MeV was useful for a fluctuation analysis.

These measurements were conducted with the 90-m WNR flight path oriented  $15^\circ$  to the primary beam. This flight path was selected to optimize the neutron energy resolution, crucial for a reliable fluctuation analysis. The detector apparatus consisted of two volume matched silicon surface barrier detectors,  $1500 \mu\text{m}$  by  $200 \text{mm}^2$ , placed at the end of the beam path. In a somewhat unusual arrangement, these detectors also provided the target material for neutron reactions on  $^{28}\text{Si}$ . ( $^{28}\text{Si}$  comprises 92% of naturally occurring silicon.) A thin sheet of lead was placed in front of each detector to prevent charged particles originating in the beam pipe from interacting in the detectors. A polyethylene radiator, placed 10 cm in front of one of the detectors, served as a neutron flux monitor.

Neutron energies were determined using standard time-of-flight (TOF) techniques. Most of the timing uncertainty was associated with the detector hardware and electronics since the source burst width was less than 1 ns. A total time uncertainty of 3 ns yielded a neutron energy resolution ranging from 10 keV at 5 MeV to 44 keV at 14 MeV. The achieved resolution is better over most of the energy range than had previously been obtained with the best of the  $(n,p)$  and  $(n,\alpha)$  measurements.

### B. $^{27}\text{Al}(d,n)^{28}\text{Si}$ measurements at Ohio University

Deuteron beams were provided by the tandem accelerator at Ohio University [6]. Deuterons comprising the primary beam were produced by a diode injector source. Chopping of the beam was accomplished by a beam deflection system driven by a sinusoidal voltage. The primary frequency was 5 MHz and an auxiliary deflection system allowed frequency selections of  $1/2^n$  ( $n=0,1,2,3,4,5,6$ ) times the primary frequency. A klystron buncher compressed the pulses to less than 1 ns duration.

A beam swinger apparatus was used to complete the neutron time-of-flight measurements. While entire angular distributions are routinely measured with this device, the swinger was fixed at  $150^\circ$  for this experiment. A scattering chamber mounted at the end of the swinger apparatus housed the targets. A target wheel with eight available target positions was placed in the chamber and aligned with the beam. The chamber was electrically insulated from the swinger, and a screen kept at  $-300$  V (relative to the chamber) suppressed electrons liberated by beam interactions. Before striking the target, the beam was collimated using a 6 mm and a 3 mm collimator. A capacitive beam pickoff located approximately 30 cm upstream from the target generated the TOF stop signal. Neutrons produced in target reactions passed through polyethylene collimators en route to the detectors located at the end of the 30 m tunnel.

Neutrons were detected with an array of six NE213 liquid scintillator detectors viewed by photomultiplier tubes. The scintillators were 17.8 cm in diameter by 2.54 cm thick. A bias of  $-2800$  volts was applied to the detectors through phototube bases using a common supply. The tube bases provided both a linear energy signal (dynode) and a fast timing signal (anode) for processing by the electronics. To minimize backgrounds produced by asynchronous gamma rays, standard pulse shape discrimination techniques were used.

To facilitate a fluctuation analysis, excitation functions for three neutron groups,  $n_2$ ,  $n_3$ , and  $n_4$ , were measured. (It was later found that the  $n_3$  group was too weakly populated to permit a reliable analysis.) The  $n_0$  and  $n_1$  groups were easily observed but the energy resolution was not good enough for a fluctuation analysis. Two factors were involved in choosing which groups to study: (1) neutron energy resolution and (2) the spacing between neighboring levels. In order to resolve an individual neutron group, the deuteron energy loss in the target must be less than the spacing between adjacent levels. It is desirable that the levels have sufficient separation to span the largest possible range in deuteron energy, requiring fewer measurements. For these reasons, it was decided to investigate the second (4.618 MeV), third (4.979 MeV), and fourth (6.277 MeV) excited states in  $^{28}\text{Si}$  with this technique. Target thickness was chosen so that the  $n_2$  and  $n_3$  groups could still be resolved at the lowest beam energy.

Since the  $Q$  value for this reaction is large and positive (9.361 MeV), it is energetically possible to explore levels at very low incident energies. However, the Coulomb barrier for deuterons (3.7 MeV) limits the practical low energy limit to around 2 MeV. To measure an excitation function, the beam energy was varied from 2.0 to 6.4 MeV in increments ranging from around 300 to 150 keV, respectively. A typical time-of-flight spectrum corresponding to a deuteron energy of 3.406 MeV depicting the neutron groups under study, is shown in Fig. 1. Note the extremely low background illustrating effective gamma ray discrimination.

### III. ANALYSIS AND RESULTS

Level densities for  $^{29}\text{Si}$  were obtained using the three methods outlined above. In the region of bound levels (i.e., excitation energies less than the neutron binding energy, 8.474 MeV), level densities were determined by a simple counting procedure using the tabulated values of Endt [7]. Average level densities evaluated at 2.677, 5.494, and 7.861 MeV were derived using this technique.

At an excitation energy just above the neutron binding energy, neutron resonance data were used to determine the level density. It can be shown that the total level density,  $\rho(E)$ , is related to the average spacing between  $1/2^+$  levels,  $\langle D_{1/2^+} \rangle$ , through

$$\rho(E) = \frac{2\sigma^2}{\langle D_{1/2^+} \rangle}, \quad (3.1)$$

where  $\sigma$  is the spin cutoff parameter. In applying this method, it is critical to be able to distinguish between  $J^\pi$  values so that a positive identification of  $1/2^+$  levels can be made. Data for this study were taken by Newson *et al.* [8] and retrieved from the National Nuclear Data Center

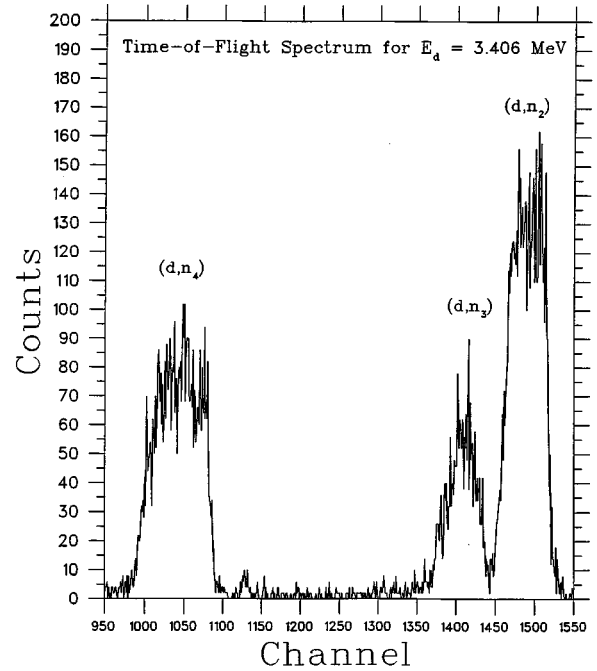


FIG. 1. Typical time-of-flight spectrum from the  $^{27}\text{Al}(d,n)^{28}\text{Si}$  measurement obtained at 3.406 MeV depicting the neutron groups under study.

(NNDC) at Brookhaven National Laboratory. These data were obtained by detecting neutrons over a 40 m flight path using neutron time-of-flight to determine the energy. Five  $s$ -wave resonances were observed in the first 1.25 MeV above the neutron binding energy of  $^{29}\text{Si}$ . The authors report uncertain spin and parity assignments for two of these levels. Under the assumption that one of the two  $1/2^+$  levels is incorrectly identified, the four remaining resonances were used to determine the level density. Spin cutoff parameters based on the single particle schemes of Seeger-Perisho [9] and Seeger-Howard [10] were calculated using the statistical mechanical code ROTHERM [11]. Spin cutoff factors calculated from the two single particle sets differ by a few percent, yielding level density values which disagree by the same amount. These results are compared with calculations in Sec. III C. However, since of the five resonances as many as two could be misidentified, the uncertainty in these results is at best 25%.

To facilitate an Ericson fluctuation analysis, excitation functions for the  $^{29}\text{Si}$  compound nucleus were measured at the two facilities described above. In the case of  $^{28}\text{Si}(n,z)$  data, level densities were inferred from excitation functions corresponding to the most prevalent charged particle exit channels:  $\alpha_0$ ,  $\alpha_1$ , and  $p_{0+1}$ . Level densities for the  $^{27}\text{Al}(d,n)^{28}\text{Si}$  experiment were determined from measured  $(d,n_2)$  and  $(d,n_4)$  excitation functions.

#### A. Reduction of $^{28}\text{Si}(n,z)$ data

In order to extract cross sections from experimental data, two-dimensional spectra of detector pulse height vs neutron time-of-flight were generated. One-dimensional energy spectra were formed by summing TOF bins corresponding to a ‘‘slice’’ in neutron energy, and projecting onto the pulse height axis. Neutron energies and bin widths were deter-

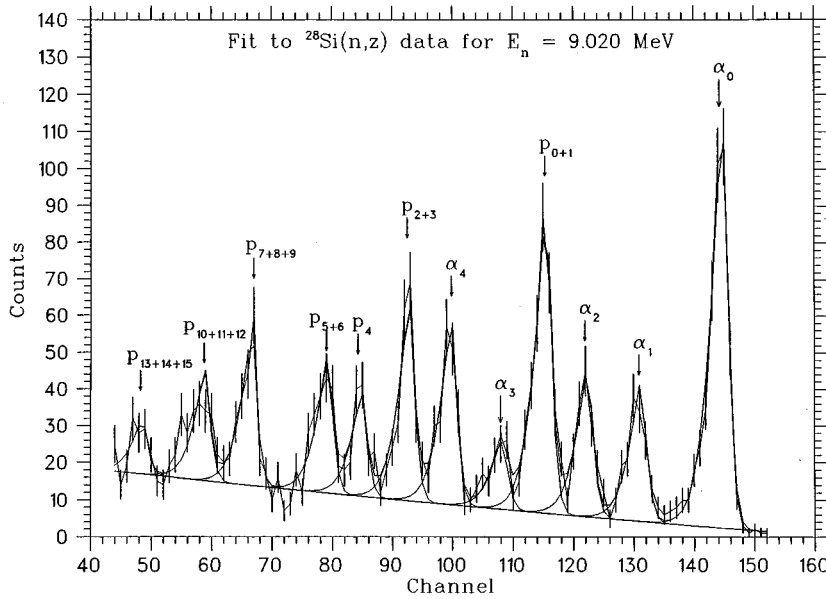


FIG. 2. Representative peak-fitting results for  $\text{Si}(n,z)$  at  $E_n=9.020$  MeV obtained using the code ALLFIT. [12].

mined from a precise time-of-flight calibration. Energy bin widths were chosen to reflect the actual experimental resolution at that energy. Since the energy of the ejected particle and residual nucleus are both deposited in the detector, the pulse height of a peak represents the total kinetic energy. However, due to the finite volume of the detector, some of the energy will be lost when a particle escapes. This is observed as a low energy tail on each peak. If an isotropic particle production throughout the active volume is assumed, it is easily shown that the fraction of particles which escape from the detector is

$$f = R \left[ \frac{r+t}{rt} \right], \quad (3.2)$$

where  $r$  is the detector radius,  $t$  is the depth, and  $R$  is the range of the particle in silicon. This factor was always less than 5% for alpha particle peaks and reached 14% for the highest energy protons.

To construct an excitation function, peaks were fit using an appropriate fitting function and the integral under each peak was used to determine the cross section. Since one spectrum exists for each neutron energy, forming an excitation function over several MeV requires fitting hundreds of spectra. Clearly, some form of automation in the fitting procedure was demanded. This task was left to the peak-fitting code ALLFIT [12]. The “standard” lineshape incorporating an asymmetric “hyper-Gaussian” flanked by two tails was chosen as a fitting function. To accommodate backgrounds, the code allows a polynomial of up to ten terms to be fitted simultaneously and subtracted from the data. Sufficiently good fits were usually obtained with a linear or quadratic fit to the background. Results of a typical fit are shown in Fig. 2. The integral under each peak returned by the fitting code was then used to calculate a partial cross section for that energy and exit channel. Absolute neutron fluences required for cross sections were obtained by integrating the recoil protons produced in the polyethylene radiator located in front of one of the detectors. The  $n$ - $p$  elastic scattering cross

sections used were from ENDF-B VI [13]. Partial cross sections were evaluated over a neutron energy range of several MeV, yielding excitation functions to be used in the Ericson analysis. Figure 3 depicts a typical excitation function for the  $(n,p_{0+1})$  channels. Observe the rapid fluctuations in the cross section with energy. Data for the  $(n,\alpha)$  channels show similar fluctuations.

### B. Reduction of $^{27}\text{Al}(d,n)^{28}\text{Si}$ data

Excitation functions for the  $n_2$  and  $n_4$  groups used in the Ericson analysis were evaluated over the bombarding energy

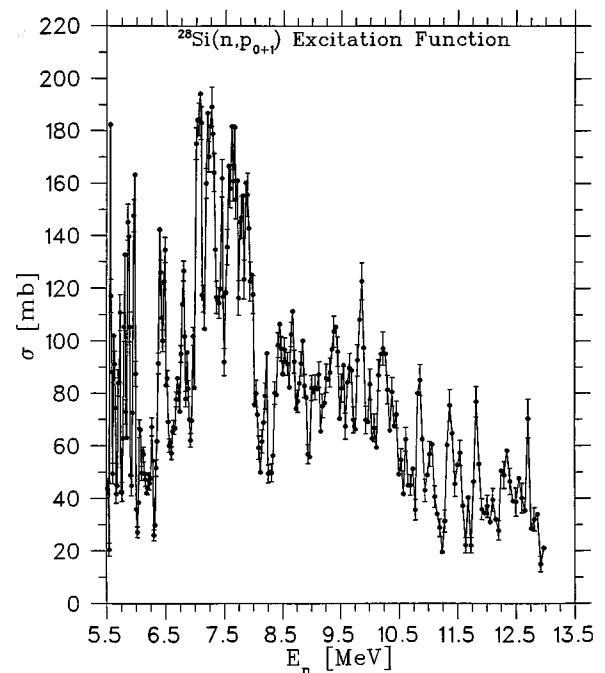


FIG. 3. Excitation function for the  $p_{0+1}$  exit channels in the  $^{28}\text{Si}(n,p)$  reaction evaluated from  $E_n=5.52$  MeV to  $E_n=12.97$  MeV. Error bars represent statistical errors only.

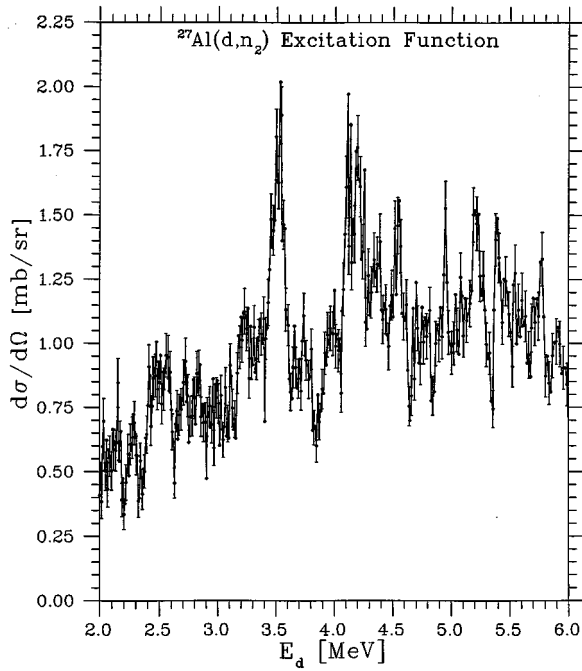


FIG. 4. Excitation function for the  $n_2$  exit channel in the  $^{27}\text{Al}(d,n)$  reaction measured from  $E_d=2.0$  MeV to  $E_d=6.0$  MeV. Error bars are based on counting statistics only.

range 2.0 to 6.0 MeV. Deuteron energies were determined from the reaction kinematics based on a precise neutron energy calibration. An accurate determination of the flight path was accomplished by fitting the positions of neutron resonances from a  $^{12}\text{C}$  transmission experiment to known resonance energies. Cross sections were obtained using the target thickness specified by the width of the TOF bin and the  $^{27}\text{Al}$  stopping power for deuterons at that energy. Backgrounds were determined by averaging the counts in a region in which there were no neutron groups, and were then subtracted from each data bin. By employing a channel-by-channel evaluation of the cross section, excitation functions were constructed with several hundred data points to be used in the fluctuation analysis. Figure 4 illustrates the excitation function for the  $n_2$  exit channel evaluated from 2.0 to 6.0 MeV.

### C. Ericson analysis

Contained in the Ericson theory are two independent techniques for determining level densities. One such approach expresses the variance of the partial cross section over a certain energy interval in terms of the average level width and level density

$$\text{var}(\sigma_{\alpha\alpha'}) = \left[ \frac{\pi\lambda^2}{(2i+1)(2I+1)} \right]^2 \frac{1}{[2\pi\Gamma\omega(E)]^2} \times \sum_{\pi} \sum_J \left[ \frac{2J+1}{H(J,\pi)} \right]^2 \sum_l \sum_{l'} (T_{\alpha l}^J T_{\alpha' l'}^J)^2, \quad (3.3)$$

where  $\alpha$  denotes the entrance channel,  $l$  the orbital angular momentum of channel  $\alpha$ ,  $i$  and  $I$  the projectile and target

spins, respectively, and  $\lambda$  the reduced wavelength of the projectile.  $J$  is the angular momentum of the compound nucleus,  $\pi$  is the parity of the compound state,  $\omega(E)$  represents the level density,  $\Gamma$  the average level width,  $T_{\alpha l}^J$  denotes the transmission coefficient for channel  $\alpha$  with angular momentum  $l$  coupled to compound spin  $J$ , and  $H(J,\pi)$  is the spin dependence of the level density given by

$$H(J,\pi) = \frac{J+1/2}{2\sigma^2} e^{-(J+1/2)^2/2\sigma^2}, \quad (3.4)$$

where it is assumed that positive and negative parity states occur with equal probability. The primed quantities have the same meaning for the exit channel. One can obtain the level density from this expression if the level width is known, the variance of the cross section is calculated from the measured cross sections, a spin cutoff factor is known [to evaluate  $H(J,\pi)$ ], and reliable transmission coefficients are available.

A second method for extracting level densities begins with an expression for transmission coefficients in terms of decay widths:

$$T_i^J = \frac{2\pi\Gamma_i^J}{D_J}, \quad (3.5)$$

where  $T_i^J$  is the transmission coefficient,  $\Gamma_i^J$  is the partial decay width of channel  $i$ , and  $D_J$  is the level spacing in the compound nucleus for level of spin  $J$ . Hence  $D_J$  is the reciprocal of the level density for a particular  $J$  and the appropriate parity. Assuming separability into spin-dependent and energy-dependent terms, the level density assumes the following product form:

$$\omega(E,J,\pi) = \omega(E)H(J,\pi) = \frac{1}{D_J}. \quad (3.6)$$

Thus if  $H(J,\pi)$  is known the value of  $D_J$  can be obtained from  $\omega(E)$ . Summing over all exit channels gives

$$\sum_i T_i^J = \frac{2\pi\sum_i \Gamma_i^J}{D_J} = \frac{2\pi\Gamma_J}{D_J}, \quad (3.7)$$

where  $\Gamma_J$  is the total width of levels of spin  $J$ . Also

$$\langle \Gamma \rangle = \sum_J P(J)\Gamma_J, \quad (3.8)$$

where the average is over all  $J$  and  $P(J)$  is the relative fraction of the cross section corresponding to compound spin  $J$  given by

$$P(J) = \frac{(2J+1)T_n^J (T_z^J/\sum_i T_i^J)}{\sum_{J'} (2J'+1)T_n^{J'} (T_z^{J'}/\sum_i T_i^{J'})}. \quad (3.9)$$

The symbol  $z$  denotes a particular charged particle exit channel and the sum over  $i$  implies all exit channels. Using the relation for  $\Gamma_J$  given in Eq. (3.7), we have

$$\Gamma_J = \frac{D_J}{2\pi} \sum_i T_i^J = \frac{1}{2\pi\omega(E)H(J,\pi)} \sum_i T_i^J. \quad (3.10)$$

Finally, substituting for  $\Gamma_J$  in Eq. (3.8) and solving for the level density gives

$$\omega(E) = \frac{1}{2\pi\Gamma} \sum_J \frac{P(J)}{H(J, \pi)} \sum_i T_i^J, \quad (3.11)$$

where  $P(J)$  is defined above. Equation (3.10) does require specific knowledge of the level densities of all residual nuclei, but only up to the maximum residual excitation energy in that decay channel. Appropriate optical model parameters must also be supplied to an optical model code to evaluate the transmission coefficients.

In order to extract a level density from the above formulas, the average level width must be determined over a certain energy interval. Several procedures exist for the determination of level widths from measured cross sections. One common method uses the autocorrelation function to derive the level width, written as

$$F(\epsilon) = \langle [\sigma(E + \epsilon) - \langle \sigma \rangle][\sigma(E) - \langle \sigma \rangle] \rangle = \frac{F(0)}{1 + (\epsilon/\Gamma)^2}, \quad (3.12)$$

where  $F(0)$  is the variance of the cross section. By evaluating this expression for various values of  $\epsilon$ , that value which makes  $F(\epsilon) = F(0)/2$  can be found. Subsequently, it was suggested [14] that  $\Gamma$  could be determined by counting the number of maxima,  $N$ , per unit energy interval in an excitation function

$$\Gamma = 0.55/N. \quad (3.13)$$

Even though this technique is the simplest to apply, often statistical fluctuations in the data can be misinterpreted as peaks and a correction for finite energy resolution is not straightforward.

An arguably more powerful technique involves expanding the excitation function in a Fourier series of the form

$$\sigma(E) = \sum_{k=0}^m a_k \cos \frac{2\pi k E}{I} + \sum_{k'=1}^m b_{k'} \sin \frac{2\pi k' E}{I}, \quad (3.14)$$

in which the number of points,  $m$ , will be  $I/d$ , where  $I$  is the energy interval to be expanded, and  $d$  is the spacing between points. The Fourier expansion coefficients  $a_k$  and  $b_k$  are independent random numbers with Gaussian distributions and therefore  $S_k = a_k^2 + b_k^2$  will have an exponential distribution. It has been demonstrated [15] that

$$S_k = a_k^2 + b_k^2 = 4\pi \frac{\Gamma}{I} \text{var}(\sigma) e^{-2\pi k \Gamma / I}. \quad (3.15)$$

Thus the level width,  $\Gamma$ , can be extracted by fitting the sum of the squares of the Fourier coefficients to the above form.

Of these three methods, Richter [16] indicates a preference for the Fourier series approach based on smaller finite range of data errors. Statistical errors in the data contribute a ‘‘white noise’’ component to the spectrum, which is independent of frequency. This effectively adds a constant to each  $S_k$ . It is therefore useful to add a constant term to the right-hand side of Eq. (3.15) in performing the fit. In addition, long range energy modulations in the cross section,

indicative of potential scattering, can affect  $\Gamma$  as well. This direct component can be excluded by ignoring the lowest order  $S_k$  values and fitting only those values beyond a certain  $S_k$ , since long range fluctuations are represented by the lowest frequency components in the Fourier expansion.

The  $S_k$  values were also compensated for the effects of finite energy resolution, following the recommendations of Grimes [17]. If a resolution function is folded into the cross section, and the Fourier expansion is calculated, the  $S_k$  values are modified in the following way:

$$S_k = f(k) S_k^0, \quad (3.16)$$

where  $S_k^0$  is the value of  $S_k$  with perfect resolution. For a Gaussian resolution function defined by

$$R(\epsilon) = \frac{1}{\sqrt{2\pi}} \frac{1}{\sigma} e^{-\epsilon^2/2\sigma^2}, \quad (3.17)$$

$f(k)$  will be

$$f(k) = e^{-(2\pi k \sigma / I)^2}. \quad (3.18)$$

The effects of finite energy resolution on the  $S_k$  values were found to be minimal in this case, with typical correction factors of only 3–4%. However, as observed by Abfalterer [18], finite resolution effects can be significant. Abfalterer applied a resolution correction to total cross section data obtained from heavier targets such as Fe. Since these targets possess smaller compound level widths, the resulting change in the  $S_k$  values was around 15%.

Average level widths were extracted from the measured cross sections using the Fourier expansion technique described above. A typical plot of  $\ln(S_k)$  vs  $k$  for the  $(d, n_2)$  channel, showing results of the fit after removal of successive  $k$  values, is given in Fig. 5. A minimum in  $\chi^2$  was obtained after the first four terms were removed. Excitation functions were evaluated over an interval chosen to be approximately 100 times the expected coherence width. The quoted error in  $\Gamma$  represents the uncertainty returned by the least-squares fitting procedure. The peak counting technique was also attempted but proved unreliable due to ambiguous peak identification. Present level width results obtained from  $(n, z)$  and  $(d, n)$  partial cross sections are compared with those of several authors in Table I [2,4,18–21]. Note that the present values compare favorably at similar excitation energies with those of other studies.

As a part of the fitting procedure for  $\Gamma$ , the constant in front of the exponential in Eq. (3.15) was also determined. This, to within a constant, is  $\Gamma \text{var}(\sigma)$  and is the parameter needed to use Eq. (3.3) to obtain the level density (variance method). Error estimates on the values of  $\Gamma$  and the product  $\Gamma \text{var}(\sigma)$  are provided by the fitting code and are typically 10%. This is an underestimate of the uncertainty because of the change in these two parameters as the cutoff value of  $k$  is changed. Examining this sensitivity suggests a value of 20% for the error in these two parameters.

A test of the appropriateness of these uncertainties was made by fitting all values of  $\Gamma$  listed in Table I with the functional form  $\alpha E^k$ . Best fit values were  $\alpha = 0.1172$  and

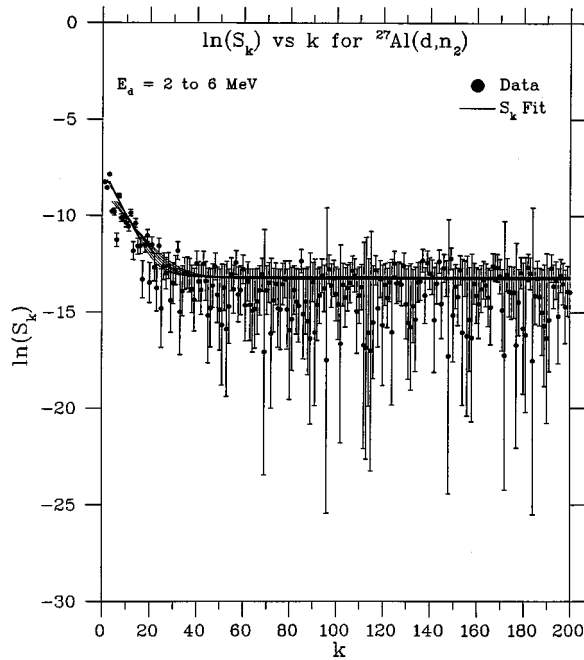


FIG. 5. Least-squares fit of  $\ln(S_k)$  vs  $k$ , where  $S_k$  is the sum of the squares of the Fourier coefficients in the expansion of the excitation function. Shown are fitting results for the  $\text{Al}(d,n_2)$  channel, upon removal of successive  $S_k$  values. A minimum in  $\chi^2$  was obtained after the first four data points were removed.

$k=2.016$ . The rms deviation of both the present points and of all points from the fitted function is consistent with an estimated uncertainty of 20%.

The values for  $\Gamma$  and for  $\Gamma\text{var}(\sigma)$  were then used with Eqs. (3.11) and Eq. (3.3), respectively, to calculate level densities of  $^{29}\text{Si}$ . Further uncertainties in the level densities beyond those due to  $\Gamma$  or  $\Gamma\text{var}(\sigma)$  are produced by the depen-

dence of Eqs. (3.3) and (3.11) on the spin cutoff factors and optical model parameters and Eq. (3.11) on the level density parameters of the residual nuclei. The uncertainty due to this latter factor is reduced by the fact that we checked these parameters in making a Hauser-Feshbach calculation of the observed average cross sections for  $(n,p)$ ,  $(n,\alpha)$ , and  $(d,n)$  reactions proceeding through the  $^{29}\text{Si}$  compound nucleus. The level density parameters were obtained from a statistical mechanical calculation of the level densities with the single particle energies of Ref. [9]. Optical model parameters used were Lawergren *et al.* [22] for deuterons, Perey and Perey [23] for protons, Rapaport [24] for neutrons, and McFadden and Satchler [25] for alpha particles.

Both the variance and width methods were applied to the  $(n,z)$  data. However, since Eq. (3.3) is only valid for angle-integrated cross sections, it was not used to determine level densities from the  $(d,n)$  data. Following the recommendations of Grimes [26], isospin corrections were applied to the optical model code which evaluates the transmission coefficients. For neutron-induced reactions on  $T=0$  targets, the coupling to the proton decay channel is reduced by 1/3. A similar reduction in the proton decay width occurs for deuteron-induced reactions on  $T=1/2$  targets. This results in a decrease in the value deduced for the level density of approximately 10%. Results of the Ericson analysis for all excitation functions are given in Fig. 6, together with values obtained from level counting and neutron resonance data. The total error on the level density points is 30%. An overall consistency of results between the two Ericson techniques and among individual excitation functions is found. Values from the present study were averaged and compared with the total cross section results of Abfalterer, Carlson, and Grimes. This comparison is shown in Fig. 7.

A least-squares fit using the Fermi gas form suggested by Gilbert and Cameron [27] was conducted using the level density results of several authors, including the present val-

TABLE I. Present level width values obtained from the Ericson analysis compared with the results of several authors.

Excitation energy (MeV)	$\Gamma$ (keV)	Reference	Reaction
14.0	24	[19]	$^{28}\text{Si}(n,\text{tot})$
14.7	24.4	[18]	$^{28}\text{Si}(n,\text{tot})$
15.4	25.1	present study	$^{28}\text{Si}(n,\alpha_0)^{25}\text{Mg}$
15.4	27.9	present study	$^{28}\text{Si}(n,p_{0+1})^{28}\text{Al}$
15.7	30.9	[18]	$^{28}\text{Si}(n,\text{tot})$
16.0	29	[4]	$^{28}\text{Si}(n,\text{tot})$ and $(n,z)$
16.3	34	[19]	$^{28}\text{Si}(n,\text{tot})$
16.4	24.1	present study	$^{28}\text{Si}(n,p_{2+3})^{28}\text{Al}$
16.5	35	[2]	$^{28}\text{Si}(n,\text{tot})$
16.8	30.5	present study	$^{28}\text{Si}(n,\alpha_1)^{25}\text{Mg}$
18.2	41	[4]	$^{28}\text{Si}(n,\text{tot})$ and $(n,z)$
18.7	41	[19]	$^{28}\text{Si}(n,\text{tot})$
19.8	46	[21]	$^{27}\text{Al}(d,p)^{28}\text{Al}$ and $^{27}\text{Al}(d,\alpha)^{25}\text{Mg}$
20.3	47	[4]	$^{28}\text{Si}(n,\text{tot})$ and $(n,z)$
21.0	44	[19]	$^{28}\text{Si}(n,\text{tot})$
21.5	44.5	present study	$^{27}\text{Al}(d,n_4)^{28}\text{Si}$
21.5	55.2	present study	$^{27}\text{Al}(d,n_2)^{28}\text{Si}$
22.3	70	[20]	$^{28}\text{Si}(n,\alpha_3)^{25}\text{Mg}$

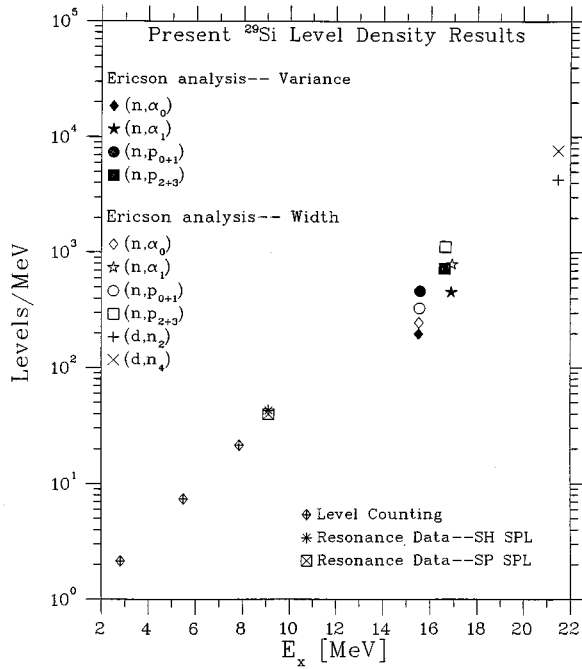


FIG. 6. Level densities obtained for  $^{29}\text{Si}$  from the Ericson analysis for all excitation functions, together with values obtained from level counting and neutron resonance data.

ues. Level density parameters obtained from the fit,  $a=3.55$ , and  $\delta=1.80$  compare well with those derived from the microscopic Fermi gas calculation,  $a=3.82$  and  $\delta=2.01$ , using Seeger-Perisho single particle levels. Results of the fit are depicted in Fig. 8.

It should be noted that inclusion of the lower energy points obtained from resonance and residual level counting is

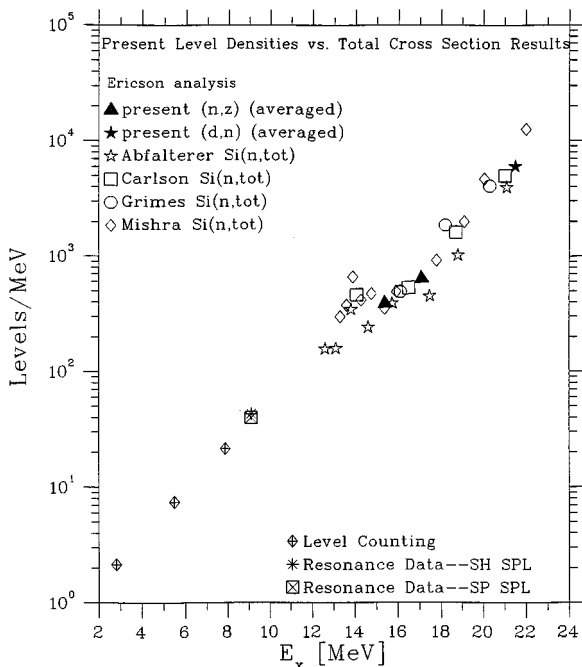


FIG. 7. Average level density values from the present study compared with the values deduced from total cross section fluctuations by Mishra, Abfalterer, Grimes, and Carlson [2,3,4,19].

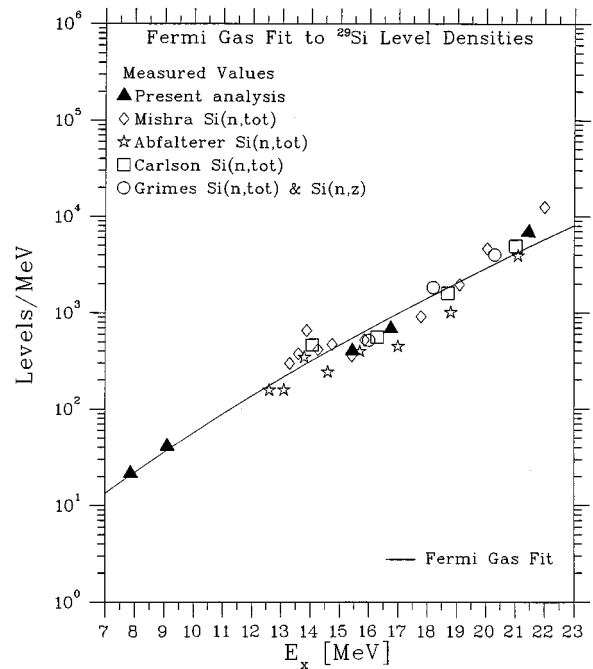


FIG. 8. A least-squares fit using the Fermi gas form suggested by Gilbert and Cameron [27] to the results of several authors, including the present values. (Symbol designations are as indicated in the legend.) [9].

very important in constraining the fit. The use of all the Ericson fluctuation points but not the points below 10 MeV would result in a fit which overestimates the level density below 10 MeV. The inclusion of only the points of Abfalterer *et al.* produces a level density which is below the combined best fit and those of Mishra *et al.* produce a level density which is above the best fit. This suggests that measurements based on total cross section data are not automatically higher or lower than those based on other data.

In order to test the experimentally determined level densities, comparisons were made to predictions of theoretical models and a number of level density compilations. Most of the compilations which exist in the literature have been efforts to develop level density systematics based on low energy resonance data. The most successful theoretical models have involved a Fermi gas approach to the level density, with enhancements to account for pairing and shell effects. In the tabulations of Gilbert and Cameron [27] and Rohr [28], level density parameters were determined by fitting a Fermi gas form of the level density to low energy resonance data. Pairing and shell effects were compensated by a pairing term,  $\Delta$ , to correct the excitation energy. In these studies, the level density parameter,  $a$ , is a constant independent of the excitation energy. Ignatyuk *et al.* [29] have proposed an energy dependent  $a$  to deal with shell and pairing effects. This alternate approach has proven fairly successful in predicting level densities over a range of mass number and excitation energy.

Level density predictions derived from compilations and theoretical models are compared with experimental values in Table II. The compilations of Rohr and Gilbert and Cameron, based on resonance data, yield comparable results. Although the predictions of Beckerman [30] are also based on



TABLE II. Level density comparison (ratio to present best fit).

Energy (MeV)	Best fit Level Density (Levels/MeV)	Seeger- Perisho (ratio)	Seeger- Howard (ratio)	Gilbert- Cameron (ratio)
5	3.4	1	2	1
10	50	1.2	3.4	1.3
15	430	1.3	3.6	1.3
20	2900	1.4	4.0	1.2
22	5800	1.6	4.3	1.3

Energy (MeV)	Rohr (ratio)	Abfalterer (ratio)	Marcazzan (ratio)	Beckerman (ratio)
5	0.9	1.8	0.6	0.7
10	1.2	1.4	0.7	0.8
15	1.3	0.9	0.7	1.0
20	1.3	0.8	0.7	1.4
22	1.4	0.7	0.7	1.7

Energy (MeV)	Ignatyuk A <sup>a</sup> (ratio)	Ignatyuk B <sup>b</sup> (ratio)
5	0.7	0.8
10	0.8	0.8
15	1.0	0.9
20	1.4	1.0
22	1.7	1.1

<sup>a</sup> $a_{\text{eff}}=4.41$ ;  $\Delta=3.09$ .

<sup>b</sup> $a_{\text{eff}}=3.86$ ;  $\Delta=2.3$ .

resonance data, the slope of the level density curve is somewhat inconsistent with experimental results and the other compilations. This is probably due to an unusual form for the level density involving a simple two-parameter exponential fit to the data. Predictions derived from the microscopic Fermi gas code RHOTHERM using the single particle energies of Seeger-Perisho and Seeger-Howard are also shown for comparison. With the exception of Beckerman, the statistical mechanical and compiled level density predictions appear to give similar slopes, although they differ in magnitude.

Level density values obtained from the results of Abfalterer *et al.* [3] and Marcazzan and Colli [31] are also presented in Table II. Both are based on previous fluctuation measurements. The fit of Abfalterer is based only on the fluctuation data obtained in Ref. [3] and low energy resonance counting; it has a flatter slope than the present data but differs from the present result by amounts which are outside of errors only at the ends of the range. The Marcazzan results are based on fluctuation measurements obtained in three different measurements but do not include low energy points obtained from level counting. The level density values of Ref. [31] are characterized by an almost identical slope but are 30% lower in magnitude than the present results. This difference could be due to the effect in Ref. [31] of either not including the low energy points or using about half as many points from Ericson fluctuation measurements.

To allow further comparison, fits of the experimental

level densities to the form of Ignatyuk *et al.* were conducted. As mentioned previously, these authors propose an energy-dependent  $a$  to compensate for shell and pairing effects. The suggested form for  $a$  is

$$a(E) = a_{\text{eff}} \left[ 1 - \frac{\Delta}{E} (1 - e^{-\gamma E}) \right]. \quad (3.19)$$

Results of two separate fits to the form of Ignatyuk are presented in Table II. (The 2.677 MeV point was excluded from the fit.) In one case,  $a_{\text{eff}}$ , the asymptotic value of the level density parameter, was held constant while the pairing and shell energy term,  $\Delta$ , was varied to optimize the fit (Ignatyuk A). The constant,  $\gamma$ , was held fixed at 0.05. The value of  $a_{\text{eff}}$  was determined using the form suggested by Ignatyuk:

$$a_{\text{eff}} = A(\alpha + \beta A), \quad (3.20)$$

where  $A$  is the mass number and  $\alpha$  and  $\beta$  are parameters as given in Ref. [29]. A fit was also made by allowing both  $a_{\text{eff}}$  and  $\Delta$  to vary (Ignatyuk B). This produced a much better representation of the data, with a 15% reduction in  $a_{\text{eff}}$ .

While discrepancies exist at the highest excitation energies, the values obtained from predictions are generally consistent with the experimental data. The predictions of Gilbert

and Cameron and Rohr, based on traditional Fermi gas methods, are in good agreement with the experimental values. The validity of the form proposed by Ignatyuk *et al.*, utilizing an energy dependent level density parameter, is also supported by the data. Poorer results are obtained from the parametrization of Beckerman and the calculation based on the levels of Seeger and Howard.

#### IV. SUMMARY AND CONCLUSIONS

A comprehensive study of the  $^{29}\text{Si}$  level density has been conducted over the excitation energy range 3 to 22 MeV using three methods. In the region of resolved levels, a simple counting procedure was used, yielding average level densities at three energies. Neutron resonance data allowed the extraction of the level density at an energy slightly above the neutron binding energy. Ericson theory was employed to deduce the level density at the highest excitation energies, by analyzing energy fluctuations in measured cross sections. Two separate experiments were conducted in order to furnish level densities in different regions of excitation. Both measurements were characterized by good energy resolution, typically 10–25 keV over the energy range studied. Excitation functions derived from  $^{28}\text{Si}(n,z)$  and  $^{27}\text{Al}(d,n)^{28}\text{Si}$  cross sections were subjected to an Ericson analysis, providing level density information from 15 to 22 MeV.

Both techniques contained in the Ericson theory were used to extract level densities. Consistency among these two techniques was observed in the values derived from the  $(n,z)$  data, lending validity to the theory. Any discrepancies between the results of the variance and width method appear to be of a random nature. Therefore it is unlikely that results of the width method could be improved by altering the residual level densities.

With the exception of the results of Beckerman, the statistical mechanical and compiled level densities appear to

give similar slopes. Clearly, the results of the statistical mechanical code, RHOTHERM, based on a microscopic Fermi gas model are extremely sensitive to the choice of single particle energies. Although the level schemes of Seeger-Perisho and Seeger-Howard differ by only a few percent, the level densities that are obtained from these input parameters can differ by a factor of 3. In the present case, the Seeger-Perisho levels give a much better representation of the experimentally determined level densities. However, this does not seem to hold in general. The results of Abfalterer [3] suggest that above  $A=40$ , the Seeger-Howard level scheme best reproduces the experimental values. The general trend of the experimental values appears consistent with the level density predictions. The consistency in the results derived from the  $(d,n)$  data, in which the gamma method was used, suggests that it can be used with confidence in cases where the variance method does not apply.

In summary, the results presented in this paper tend to validate the conventional Fermi gas form of the level density and the techniques of Ericson analysis. Ericson fluctuation theory was shown to yield level densities satisfactorily in the region of overlapping levels, showing consistency between different reactions and between the two techniques of analysis. With the inclusion of the present results, a quite comprehensive database exists for  $^{29}\text{Si}$  over a range of excitation energy. The present study suggests that for a particular nucleus, a wealth of available data allows a fairly accurate determination of the level density. It is hoped that these results will encourage further investigation of other nuclei so that a consistent picture of level densities emerges.

#### ACKNOWLEDGMENTS

This work was supported by the U.S. Department of Energy under Contract Nos. DE-FG02-88-ER40387 and W-7405-ENG-36.

- 
- [1] T. Ericson, Phys. Rev. Lett. **5**, 430 (1960); Ann. Phys. (N.Y.) **23**, 340 (1963).
  - [2] V. Mishra, N. Boukharouba, S. M. Grimes, K. Doctor, R. S. Pedroni, and R. C. Haight, Phys. Rev. C **44**, 2419 (1991).
  - [3] W. Abfalterer, R. W. Finlay, S. M. Grimes, and V. Mishra, Phys. Rev. C **47**, 1033 (1993).
  - [4] S. M. Grimes, Nucl. Phys. **A124**, 369 (1969).
  - [5] H. Condè, R. C. Haight, H. Klein, and P. Lisowski, *Proceedings of the International Conference on Nuclear Data for Science and Technology*, Jülich, Germany, 1991, edited by S. M. Qaim (Springer-Verlag, Berlin, 1992), p. 386.
  - [6] D. E. Bainum, Ph.D. dissertation, Ohio University, 1977.
  - [7] P. M. Endt, Nucl. Phys. **A521**, 1 (1990).
  - [8] H. W. Newson, W. F. E. Pineo, B. H. Choi, J. M. Clement, and M. Divadeenam, Ann. Phys. (N.Y.) **103**, 121 (1977).
  - [9] P. A. Seeger and R. C. Perisho, Los Alamos Scientific Laboratory Report No. LA-3751, 1967.
  - [10] P. A. Seeger and W. M. Howard, Nucl. Phys. **A238**, 491 (1975).
  - [11] S. M. Grimes, J. D. Anderson, J. W. McClure, B. A. Pohl, and C. Wong, Phys. Rev. C **10**, 2373 (1974).
  - [12] J. Kelly, private communication.
  - [13] G. M. Hale, D. C. Dodder, E. R. Siciliano, and W. B. Wilson, "ENDF-B VI Evaluation for Neutron Interactions with  $^1\text{H}$ ," National Nuclear Data Center, Brookhaven National Laboratory Report MAT-125, 1989.
  - [14] D. M. Brink and R. O. Stephen, Phys. Lett. **5**, 77 (1963).
  - [15] M. Böhning, Jahresber. (Max Planck Institut für Kernphysik), Heidelberg, 105 (1965).
  - [16] A. Richter, in *Nuclear Spectroscopy and Reactions*, edited by J. Cerny (Academic, New York, 1974), Pt. B, pp. 343–391.
  - [17] S. M. Grimes, Ohio University Internal Report INPP 95-01 1995.
  - [18] W. Abfalterer, Ph.D. thesis, Ohio University, 1995.
  - [19] A. D. Carlson and H. H. Barschall, Phys. Rev. **158**, 1142 (1967).
  - [20] L. Papineau, Saclay Report CEA R-2876, 1966.
  - [21] M. Corti, M. G. Marcuzzan, M. Milazzo, and L. Colli Milazzo, Nucl. Phys. **77**, 625 (1966).
  - [22] B. Lawergren, G. C. Morrison and A. T. G. Ferguson, Nucl. Phys. **A106**, 2 (1968).

- [23] C. M. Perey and F. G. Perey, *At. Data Nucl. Data Tables* **13**, 293 (1974).
- [24] J. Rapaport, *Phys. Rep.* **87**, 27 (1982).
- [25] L. McFadden and G. R. Satchler, *Nucl. Phys.* **84**, 177 (1966).
- [26] S. M. Grimes, *Phys. Rev. C* **46**, 1064 (1992).
- [27] A. Gilbert and A. G. W. Cameron, *Can. J. Phys.* **43**, 1446 (1965).
- [28] G. Rohr, *Z. Phys. A* **318**, 299 (1984).
- [29] A. V. Ignatyuk, G. N. Smirenkin, and A. S. Tishin, *Yad. Fiz.* **21**, 485 (1975) [*Sov. J. Nucl. Phys.* **21**, 255 (1975)].
- [30] M. Beckerman, *Nucl. Phys.* **A278**, 333 (1977).
- [31] G. M. Braga-Marcazzan and L. Milazzo-Colli, *Energ. Nucl. (Italy)* **15**, 186 (1968).